Numerical simulations of groundwater age in discretely fractured porous rock

J. W. Molson
Canada Research Chair in Quantitative Hydrogeology of Fractured Media
Université Laval, Dept. of Geology & Geological Engineering
Québec, Québec G1V 0A6 (418) 656-5713 john.molson@ggl.ulaval.ca
E. O. Frind
Professor Emeritus, University of Waterloo, Dept. of Earth & Environmental Sciences,
Waterloo, Ontario, Canada N2L 3G1 frind@uwaterloo.ca

ABSTRACT
A three-dimensional numerical model for simulating groundwater residence time (age) within fractured porous rock is developed and applied. The model considers advective-dispersive age transport within a discretely-fractured porous medium, and includes age diffusion into (or out of) the porous matrix. The model is applied to two examples of discretely fractured porous rock. The results show strong age gradients along fracture-matrix interfaces, with multiple fracture pathways containing groundwater of different age. Mixing of waters of different age leads to the establishment of steady-state age throughout most of the system. In these types of hydrogeological environments, complex fracture pathways play critical roles in determining groundwater age distributions.

RÉSUMÉ
Un modèle numérique tridimensionnel d'un aquifère poreux avec des fractures discrètes a été développé pour simuler le temps de résidence (l'âge) des eaux souterraines dans un tel milieu. Ce modèle peut simuler les processus d'advection et de dispersion en fonction du temps ainsi que le phénomène de diffusion dans la matrice poreuse. Il a été appliqué à deux exemples de milieux poreux fracturés. Les résultats obtenus démontrent que des gradients importants d'âge des eaux souterraines se produisent le long des interfaces des fractures et qu'ils existent plusieurs voies de transport des eaux souterraines d'âges variables. Dans ce type de système hydrogéologique, des voies complexes de transport et la dispersion jouent des rôles critiques au niveau de la distribution de l'âge des eaux souterraines.

1 INTRODUCTION

Fractured rock aquifers are increasingly being relied upon as drinking water sources for many communities. However, these complex hydrogeological systems are often vulnerable to contamination and notoriously difficult to characterize. Better characterization and interpretation methodologies are required to manage these resources and ensure their sustainability.

Groundwater age is a critical parameter in many field site investigations involving protection, sustainability and remediation of fractured rock aquifers. Older water, for example, may indicate a less vulnerable water source, but if over-pumped, the source may not be sustainable. Younger, or more recently recharged water, implies more direct fracture pathways to ground surface which would suggest a higher vulnerability. Groundwater age is also important for interpreting flow paths and watershed-scale geochemical evolution, identifying surface water - groundwater interactions, estimating historical recharge rates, and for assessing site suitability for nuclear waste disposal.

Groundwater age in porous media can be simulated using a variety of methods, including analytical solutions (e.g. Bethke and Johnson, 2002; Chesnaux et al., 2006; Braunsfurth and Schneider, 2008), direct age simulations using numerical methods (Goode, 1996; Engesgaard and Molson, 1998; Cornaton and Perrochet, 2002; Molson & Frind, 2005), particle tracking (e.g. Molson & Frind, 2005), and indirectly using analytical or numerical mass transport modelling (e.g. by simulating isotope transport and decay; see Cook et al. 2005). In comparisons of advective age predictions with direct age and ^{14}C-age simulations, Castro and Goblet (2005) show that the direct approach is superior. To date, these methods have been applied almost exclusively to porous media while applications to fractured media have been rare.

In this study, a new finite element numerical model is developed to gain insight into how groundwater age evolves within active flow networks in fractured porous media. The original motivation for the study came from observed natural thermal anomalies in a fractured dolostone (Pehme et al., 2007). In the proposed conceptual model, weak but distinct thermal anomalies observed within lined boreholes were thought to originate from active fractures carrying groundwater which had recharged at different times and were thus at different temperatures when they reached the observation well. A more complete picture of the age distribution within the fracture network was required to confirm the conceptual model.

The objective here is to introduce the modelling approach, to highlight its potential use for simulating and interpreting groundwater age distributions within discretely fractured porous rock systems, and to show how a steady-state age distribution can be attained in such systems.

2 SIMULATION APPROACH

In this study, the three-dimensional (3D) discrete fracture network (DFN) model HEATFLOW (Molson et al. 1992, Molson and Frind, 2008; Molson et al., 2007) is modified to simulate groundwater age.

The HEATFLOW model solves the governing equations for groundwater flow and advective-dispersive transport through both a porous and permeable matrix and a discrete fracture network. We assume a saturated medium, negligible density gradients and planar fractures.

2.1 Governing equations

The advective-dispersive age transport equation for the porous matrix can be expressed as :

$$\frac{\partial}{\partial x_i}\left[D_{ij}\frac{\partial A}{\partial x_j}\right]-v_i\frac{\partial A}{\partial x_i}+1=\frac{\partial A}{\partial t} \qquad [1]$$

where A is the groundwater age (days), D_{ij} is the hydrodynamic dispersion tensor (m^2d^{-1}), v_i is the average linear groundwater velocity (md^{-1}) (determined from the hydraulic head solution), x_i are the spatial coordinates (m) and t is time (days). Following the definition given by Goode (1996), equation (1) is derived from the conservation of age-mass.

The governing equation for groundwater age within a planar fracture can be written as:

$$\frac{\partial}{\partial x_i}\left(D'_{ij}\frac{\partial A'}{\partial x_j}\right)-\overline{v}_i\frac{\partial A'}{\partial x_i}-\frac{D_{ij}}{b}\left[\frac{\partial A}{\partial z}\right]_{z=\pm b}+1=\frac{\partial A'}{\partial t} \qquad [2]$$

where A' is the age of groundwater within the fracture (days), D'_{ij} is the hydrodynamic dispersion tensor for the fracture (m^2d^{-1}), $\overline{v}_i$ are the fracture velocities (md^{-1}), and b is the half-fracture aperture (m). The second-last term on the left hand side of (2) represents the dispersive age transfer between the fracture and the porous matrix.

The term +1 in equations (1) and (2) represent age source terms which increase the groundwater age at a rate of +1 day/day (Goode, 1996). As water recharges across an inflow boundary, it is assigned a reference age of A=0 days. Within the domain, the groundwater will age at +1 day/day everywhere, but because of inflow of young water, as well as variable flow velocities (e.g. fractures vs. matrix) and dispersion, the age will evolve in distinct patterns. As a consequence, the groundwater age at certain points can stabilize in time as we will demonstrate below.

The fracture velocities for equation (2) are determined in the model using the simulated hydraulic head field and using the cubic law which can be written as:

$$\overline{v}_i=\frac{-(2b)^2}{12\mu}\rho g\nabla h \qquad [3]$$

where $2b$ is the full fracture aperture (m), μ and ρ are the viscosity ($kgm^{-1}s^{-1}$) and density (kgm^{-3}) of water, respectively, g is the gravitational acceleration (ms^{-2}) and ∇h is the hydraulic head gradient (-). For example, assuming a gradient $\nabla h=0.01$, 2b=200 μm (2×10^{-4} m), ρ=1000 kg/m^3, μ=10^{-3} Pa·s, then v = 0.00033 m/s, or ~29 m/d.

Boundary conditions for the systems of equations (1) and (2) include the standard first, second or third-type (Molson and Frind, 2005). The initial condition is A=0 and the model is run to steady state.

2.2 Solution Methodology

Equations (1) and (2) are solved simultaneously using a finite element approach with 3D rectangular prism elements for the porous matrix and 2D elements for the fractures. The fracture elements are embedded directly into the porous medium. The model includes a corresponding 3D groundwater flow solver for computing hydraulic heads and groundwater flow velocities in the matrix and fractures. Further details are provided in Molson et al. (1992) and Molson & Frind (2008).

3 MODEL APPLICATIONS

3.1 Simplified 4-Pathway Model

We begin with a relatively simple 2D vertical section conceptual model with 4 discrete fracture pathways between the surface inflow boundary and an exit boundary receptor. The conceptual model and flow boundary conditions are shown in Figure 1.

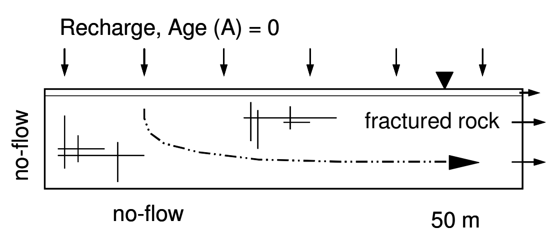

Figure 1. Conceptual model for the advective-dispersive age simulations in fractured media.

The system measures 500 x 50 m and is resolved using 500 x 50 elements. The top boundary represents the watertable. For clarity, only the upgradient half of the domain is shown (0-250 m). A 2 m thick homogeneous non-fractured layer (K=10^{-5} m/s) is placed across the top in order to naturally distribute the surface recharge into the fractures. Excess water not able to infiltrate the underlying rock is allowed to discharge out the right boundary (similar to runoff). All fractures have a uniform aperture of 200 μm.

The flow system is defined using no-flow boundaries at the left and bottom boundaries and a fixed head at the right outflow boundary (at x=500 m). A recharge rate of 5 cm/yr is assigned across the top surface. The groundwater age is fixed at A=0 across the upper recharge boundary while zero age-gradient conditions are assigned along all other boundaries. All physical parameters are given in Table 1.

Table 1. Physical model parameters for the groundwater age simulations.

Parameter	**Value**
Matrix hydraulic conductivity	10^{-8} m/s
Matrix porosity	0.10
Recharge rate	5 cm/yr
Dispersivities	
- longitudinal	0.1 m
- transverse vertical	0.01 m
Diffusion coefficient	1.6×10^{-9} m^2/s
Fracture statistics (DFN)(1)	(vertical, horizontal set)
- mean aperture 2b	200, 200 μm
- mean spacing	5, 2.5 m
- mean length	10, 50 m

(1) Fracture statistics apply to the random discrete fracture network (uniform apertures of 200 μm were assumed for the 4-pathway model).

The time stepping simulation starts at t=0 with an initial condition of A=0. As expected, age increases everywhere as the water initially in the system ages, and new water entering with an age of A=0 also ages. But because water moves faster in the fractures, fracture water will always be younger than the neighboring matrix water. Mixing between the two eventually leads to a steady-state age.

For the given system, an essentially steady-state age distribution is reached at about 200 years. Figure 2 shows the heads, the velocities in the fractures, and the age distribution at steady state. While the hydraulic heads show general flow gradients downwards and to the right (Figure 2a), the velocity field (Figure 2b) shows that transport will be primarily controlled by the fractures, where the velocities are on the order of 10 m/day (rock matrix velocities are about 3-4 orders of magnitude less).

The simulated steady-state age distribution shows the youngest water within the top high-K layer, with the fractures serving as rapid conduits for migration through the low-K rock (Figure 2c). While rapid advective transport through the fractures carries young water deep within the system, the fracture water nevertheless ages considerably along the migration path. This is especially evident within the deepest and longest pathways furthest upgradient.

As the relatively immobile matrix water ages, dispersive mixing will transfer age from the matrix to the fractures. Thus, by the time the fracture water reaches the downgradient limit at x=250 m, its age has increased to 63, 30, 16 and 8 years for the four fracture pathways, from longest to shortest, respectively (Figure 3). In comparison, under purely advective transport alone, the age of groundwater at the downgradient limit of the longest fracture pathway (~240 m, migrating at a rate of ~10 m/d), would be on the order of 24 days. Similar effects of matrix diffusion on groundwater age are shown by Cook et al. (2005) using mass transport simulations.

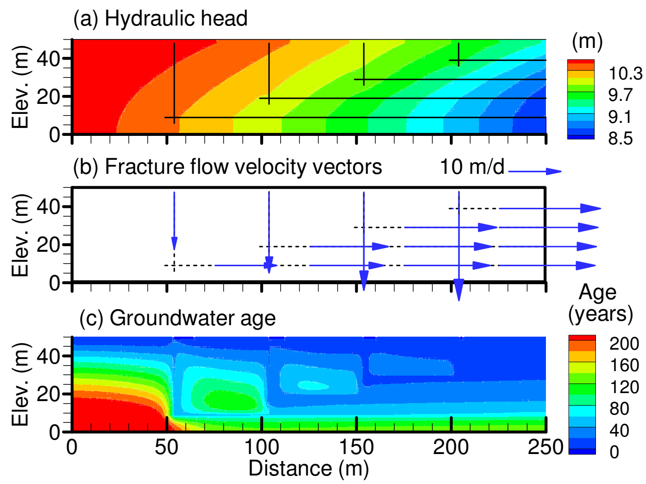

Figure 2. Simulated steady-state results from the 4-pathway model showing (a) hydraulic heads, (b) fracture flow velocities and (c) groundwater age. Velocities apply at vector tail points (not all are shown). Matrix velocities are orders of magnitude less, thus are not shown.

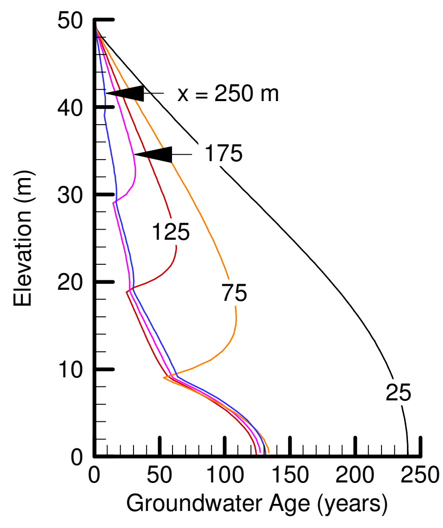

Figure 3. Simulated steady-state vertical age profiles from the simplified 4-pathway model at selected locations (at x=25 m, mid-way between each of the vertical fractures, and at x=250 m). Local age minima correspond to fracture intersections.

While these simulation results apply to a simplified fracture system with uniform 200 μm apertures, it is clearly evident that even along otherwise rapid fracture pathways, “dispersive ageing” of groundwater within the fractures can be significant.

3.2 Random Fracture Network

In the second conceptual model, we use the same basic geometrical domain, grid and boundary conditions as in the simplified case above, but add a random discrete fracture network into the porous medium. Three cases will be presented (A, B & C), each with a different matrix hydraulic conductivity, but otherwise identical.

Two orthogonal sets of planar fractures make up the fracture network: one in the horizontal (x,y) plane, the other in the vertical transverse (y,z) plane. Each set is characterized by a mean and standard deviation for fracture length, aperture, and spacing (Table 1).

The simulated flow systems and steady-state age distributions are provided for Cases A ($K_{matrix}=10^{-8}$ m/s), B ($K_{matrix}=10^{-7}$ m/s) and C ($K_{matrix}=10^{-9}$ m/s) in Figures 4, 5 and 6, respectively. Selected vertical age profiles are shown in Figure 7.

As in the above simplified case, essentially steady-state age distributions are reached after about 200 years, with time to steady state increasing somewhat as the matrix K is reduced.

In the base case simulation (Case A), the flow field is characterized by the expected horizontally dominant flow gradients with some significant vertical connectivity (Figure 4a & b). Flow is again focussed through the active fractures, with stagnant (low-flow) zones within the matrix blocks between the fractures. Stagnant zones are particularly evident near the lower left boundary and along the lower boundary between 160 m and 200 m.

The simulated age distribution (Figure 4c & d) is consistent with the flow field, with age generally increasing with depth and being highest within the stagnant or low-flow zones. Maximum groundwater ages of between approximately 50-100 years are reached along the lower boundary. A groundwater age of ~200 years is located at the lower left stagnation point, however this local value will keep increasing with the simulation time while the rest of the domain remains at steady state.

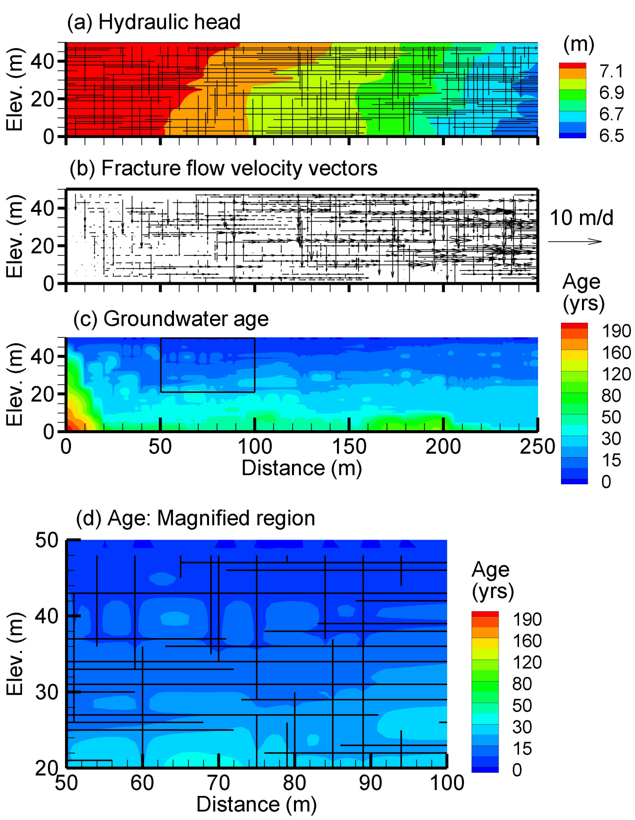

Figure 4. Case A ($K_{matrix}=10^{-8}$ m/s): Simulated steady-state results from the random fracture network model showing (a) hydraulic heads, (b) fracture flow velocities and (c & d) groundwater age (magnified region in 4d is highlighted by box in 4c). For clarity, not all vectors are shown in Figure 4b.

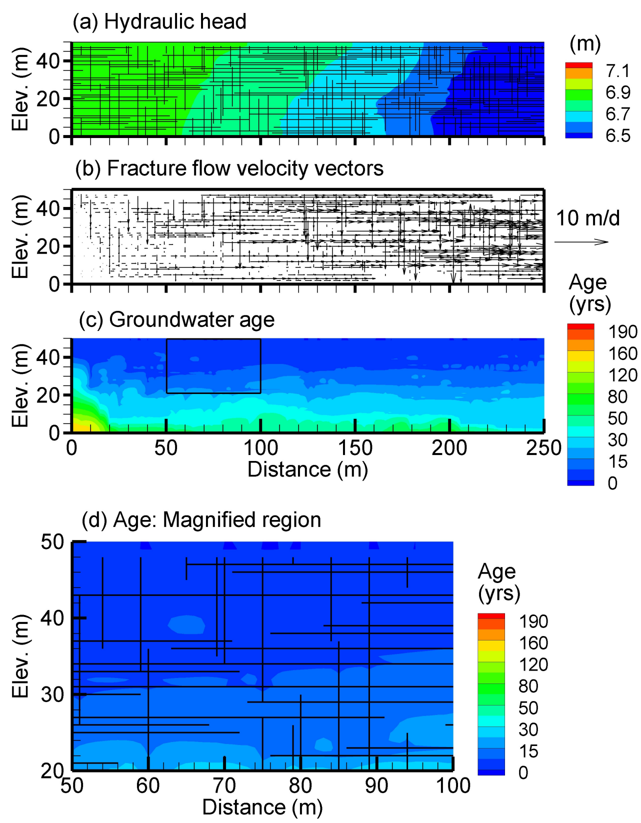

Figure 5. Case B ($K_{matrix}=10^{-7}$ m/s): Simulated steady-state results from the random fracture network model showing (a) hydraulic heads, (b) fracture flow velocities and (c & d) groundwater age.

Increasing the matrix hydraulic conductivity (K) to 10^{-7} m/s (Case B, Figure 5) has the expected effect of lowering the hydraulic gradient. However, the K contrast between the upper 2m-thick homogenous layer and the underlying rock is now less. Thus compared to the previous case, proportionately more water flows through the underlying fractured rock system, and proportionately less water discharges out the right boundary of the high-K surface layer.

A greater flux of younger recharge water thus enters the fractures (and some through the now more permeable matrix), which reduces the groundwater age relative to Case A. The age distribution is generally smoother, with noticeably fewer isolated matrix blocks containing older water.

Conversely, on decreasing the matrix K to 10^{-9} m/s (Case C, Figure 6), the flux of young recharge water that enters the fractured rock system is reduced and the groundwater age increases relative to the base case (Case A). The age distribution in Case C is also more irregular, resulting from a greater age contrast between the younger groundwater in the fractures and the older water within the isolated low-K matrix blocks.

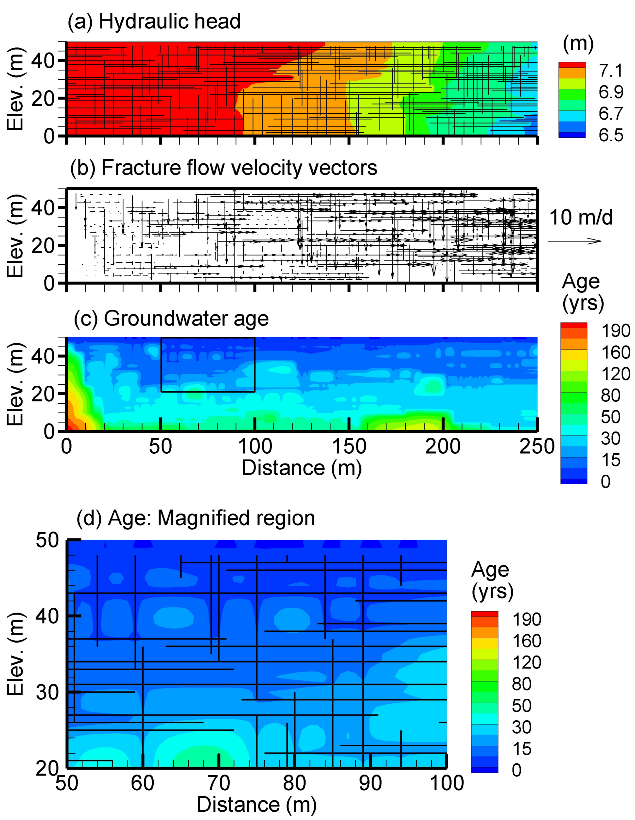

Figure 6. Case C ($K_{matrix}=10^{-9}$ m/s): Simulated steady-state results from the random fracture network model showing (a) hydraulic heads, (b) fracture flow velocities and (c & d) groundwater age.

The vertical age profiles for all 3 cases also reflect the trend of increasing age with depth, with local fracture-induced perturbations (Figure 7). Note that although age generally increases with depth, it does not generally increase with distance downgradient.

In a homogeneous porous medium, dispersive ageing will occur in a relatively uniform manner and age will predictably increase along well-defined flowlines (e.g. see Molson and Frind, 2005). In complex fracture networks, however, there will be more complex mixing patterns where, for example, older deeper water may be forced upwards around a stagnation zone where it will rapidly mix with younger recharge water. In the present cases, the mixing between the younger water flowing vertically downward through the fractures with the older water moving horizontally in the fractures (or diffusing from the matrix) is sufficient to balance the ageing process, with the result that very little increase in age is observed in the longitudinal direction along the section.

Thus, as in the simplified case above, originally young recharge water migrating rapidly through active fracture networks can become significantly older due to dispersive mixing with older groundwater within matrix stagnation zones.

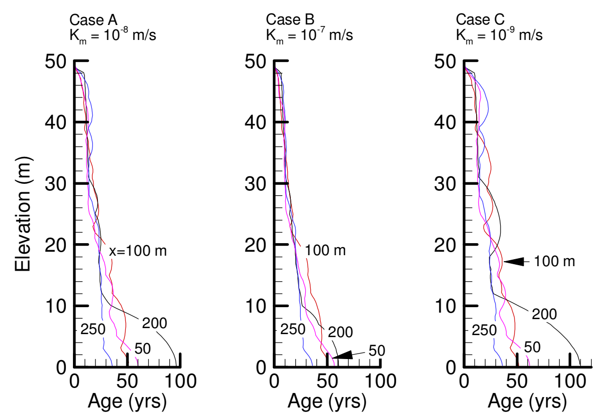

Figure 7. Simulated vertical age profiles at selected distances (x) downgradient, for (a) Case A, (b) Case B and (c) Case C.

4 CONCLUSIONS

The simulated age distributions have shown that mixing along fracture interfaces of young recharge water with older matrix water can significantly increase the age of groundwater within the fractures. This dispersive ageing results in much older fracture water than would be expected based on rapid advective transport alone.

Furthermore, the local-scale depth-dependent age differences within these simulated fracture networks are at least on the order of several months and often on the order of several years, even for relatively rapid fracture flow paths.

This work is leading to new insights into the possible origins of natural thermal anomalies observed within fracture rock. The direct age simulations are currently being correlated with advanced thermal transport modelling within these same types of discrete fracture systems. The aim is to help characterize active fracture networks and improve our conceptual models of these complex hydrogeological systems.

ACKNOWLEDGEMENTS

This research was financially supported by the Canada Research Chair in Quantitative Hydrogeology of Fractured Porous Media, held by the first author at Université Laval. Computational resources were provided in part from a CFI award to the first author, as well as by Environment Canada (with D. Van Stempvoort and G. Bickerton) through a research contract funded by PERD (Program of Energy Research and Development).

REFERENCES

Bethke, C.M. and Johnson, T.M. 2002. Paradox of groundwater age. *Geology* 30(2): 107–110.

Braunsfurth, A.C. and Schneider, W. 2008. Calculating ground water transit time of horizontal flow through leaky aquifers, *Ground Water* 46(1): 160-163.

Castro, M.C., and Goblet, P. 2005. Comparison of groundwater ages – A comparative analysis. *Ground Water* 43(3): 368-380.

Chesnaux, R., Molson, J.W., Chapuis, R. 2005. An analytical solution for ground water transit time through unconfined aquifers, *Ground Water* 43(4): 511-517.

Cook, P.G., Love, A.J., Robinson, N.I., and Simmons, C.T. 2005. Groundwater ages in fractured rock aquifers, *Journal of Hydrology*, 308: 284-301.

Cornaton, F. and Perrochet, P. 2002. Direct mathematical method for the computation of groundwater age and transit time distributions in reservoirs, including dispersion processes. *Acta Universitatis Carolinae—Geologic*a 46(2/3): 58–61.

Engesgaard, P. and Molson, J.W. 1998. Direct simulation of groundwater age in the Rabis Creek aquifer, Denmark. *Ground Water* 36(4): 577–582.

Goode, D. 1996. Direct simulation of groundwater age. *Water Resour. Res*. 32(2): 289–296.

Molson, J.W., and Frind, E.O. 2008. *HEATFLOW: A 3D groundwater flow and thermal energy/mass transport model for porous or discretely fractured porous media*, version 3.0, University of Waterloo.

Molson, J.W. and Frind, E.O. 2005. How old is the water? Simulating groundwater age at the watershed scale, Abstract and paper: *Bringing Groundwater Quality Research to the Watershed Scale,* In: *Proceedings of GQ2004, the 4th International Groundwater Quality Conference* (N. Thompson, Ed.), Waterloo, Canada, July 2004. IAHS Publ. 297, p. 482-488.

Molson, J.W., Frind, E.O., and Palmer, C. 1992. Thermal energy storage in an unconfined aquifer 2. Model development, validation and application, *Water Resources Research*, 28(10): 2857-2867.

Molson, J.W., Pehme, P., Cherry, J., and Parker, B. 2007. Numerical analysis of heat transport in fractured sedimentary rock: Implications for thermal probes, In Proceedings: 2007 NGWA/U.S. EPA Fractured Rock Conference: State of the Science and Measuring Success in Remediation (#5017), Portland, Maine, September 24-26.

Pehme, P., Greenhouse, J.P. and Parker, B.L. 2007. The Active Line Source temperature logging technique and its application in fractured rock hydrogeology, *Journal of Environmental and Engineering Geophysics* 12, no. 4: 307-322.